

Analysis of adaptive higher order exponential variational integrators

Odysseas Kosmas

Modelling and Simulation Centre, Department of Mechanical, Aerospace and Civil Engineering, The University of Manchester, George Begg Building, M1 3BB Manchester, UK

Abstract: Variational integrators are powerful tools for advanced numerical solutions of mechanical problems appeared in mathematics and physical sciences. Compared to standard schemes they may be applied to complex systems where the computational cost is very high. In the present paper, we make an attempt to explore whether their methodology may be effective in adaptive time step variational integrators with the use of the space-time geodesic approach of classical mechanics while being combined with a simultaneous decrease, as much as possible, of the corresponding cost. Following the advantages of our previously deduced variational integrators, we now formulate a derivation of time adaptive high order exponential variational integrators. As a first step, this is successfully achieved for systems of which their Lagrangian is of separable form. Towards this end, we start from unfolding the standard Euler-Lagrange system to its space-time manifold and then we rewrite it as a geodesic problem with zero potential energy. Simulation results, without the need to optimise the step size, show that one can employ the space-time geodesic formulation to generate an adaptive scheme that still preserves general underlying geometric structure properties of the system

Keywords: Variational integrators, High order geometric integrators, Discrete variational mechanics, Highly oscillatory problems, General N-body problem

Date of Submission: 06-10-2020

Date of Acceptance: 19-10-2020

I. INTRODUCTION

In recent years, many scientific phenomena are investigated by computer models and codes which are remarkably complex. Computational experiments, i.e. runs of these codes executed with various input data, make predictions (through the provided output) of several physical observables and parameters. In most of the cases the runs are computationally expensive and often our objective is the required computer experiments to be less time consuming predictors of the output for a specific data.

In the special case when solving ordinary differential equations (ODEs) using numerical integration schemes, in order to reduce computational cost, the time adaptivity is a key ingredient (Marsden et al., 1998; Hairer, 1997). Admittedly this tool possesses significant advantages with respect to the efficiency, the computational accuracy, and the ease in the implementation. Although time adaptivity performs remarkably well in many applications for problems involving the integration of Hamiltonian systems, the use of symplectic integrators has been well established (Kane et al., 1999; Leok and Zhang, 2011; Bloebaum and Saake, 2015).

During the past few decades many authors have addressed various derivations and have adopted symplectic integrators with variable time steps, despite the fact that the early results were not quite promising (Skeel, 1993; Calvo and Sanz-Serna, 1993; Wright, 1998). Essentially, two main types of time variation steps have been utilized. In the first type the time step was explicitly varied in the flow of the time, a choice mostly resulting to problems, while in the second, the time step was chosen while using the dynamical variables of the system, namely particle positions q and corresponding momenta p . For the case of the variable time, the derived equations are no longer in canonical Hamiltonian form, a fact that makes the obtained results rather unreliable.

The aforementioned shortcomings may be reduced if an adaptive time step integrator frame, that uses a high order non-symplectic scheme, will be adopted (Hairer, 1997; Reich, 1999, Marsden and West, 2001; Stern and Grinspun, 2009). In our present work, we improve the Galerkin type high order integrators of (Kosmas and Vlachos, 2010; Kosmas and Leyendecker, 2016; Kosmas and Leyendecker, 2019) in such a way that adaptive time stepping will be used. In addition to the space-time approach of (Marsden et al., 1998; Kane et al., 1999), the geodesic view point of (Nair, 2012; Kosmas and Vlachos, 2016) is regarded which provides the possibility to overcome problems that appear when symplectic integrators with variable time steps are utilized. One of our goals is to derive an optimal time-step adaptation method computationally cheaper as much as possible (Kosmas and Leyendecker, 2012; Kosmas, 2011; Kosmas, 2019; Kosmas and Leyendecker, 2015, Kosmas and paqpadopoulos, 2014).

Towards this end, we first formulate the combined space-time and geodesic ideas of adaptive time stepping (Section 2) in connection with the exponential variational integrators (Section 3). Then, the proposed methods are presented in Section 4 and tested in a couple of numerical applications in Section 5. Finally, the advantages of the derived method are summarized in Section 6.

II. THE GEODESIC APPROACH IN DERIVING TIME ADAPTIVE INTEGRATORS

In order to derive time adaptive integrators, we start from the continuous Lagrangian formulation and consider physical problems described through Lagrangian functions of the form

$$L(x, \dot{x}) = \frac{1}{2} \dot{x}^2 - V(x), \quad x \in \mathbb{R} \quad (1)$$

The corresponding Euler-Lagrange equation is the second order differential equation

$$\ddot{x} = \frac{\partial V}{\partial x} \quad (2)$$

where, as usually, dots represent time derivatives. By choosing the initial conditions as $x_0 = x(0)$ and $\dot{x}_0 = \dot{x}(0)$, an expression of $x(t)$ can be determined and adopted for some time interval $t \in [0, T]$, as a solution of (1).

We then consider the Lagrangian

$$\tilde{L} = \frac{1}{2} x'^2 + \frac{1}{2V} t'^2 \quad (3)$$

where the primes denote differentiation with respect to some parameter λ , see (Kosmas and Vlachos, 2016). For the latter Lagrangian the corresponding Euler-Lagrange equations and the relevant initial conditions take the form

$$x'' = -\frac{1}{2V^2} x'^2 + \frac{1}{2V} t'^2 \quad \text{for} \quad x_0 = x(0), \quad x'_0 = \dot{x}(0)t'_0, \quad (4a)$$

$$t'' = -\frac{1}{V} \frac{\partial V}{\partial x} t' x' \quad \text{for} \quad t_0 = 0, \quad t'_0 = aV(x_0). \quad (4b)$$

It is worth mentioning that, even though \tilde{L} depends upon V and couples the space and time variables in a non trivial manner, the evolution equations for x depend only on $\frac{\partial V}{\partial x}$. Furthermore, we note that one could add on V any constant without changing the x -dynamics (Nair, 2012; Kosmas and Vlachos, 2016).

We now consider two functions of the parameter λ , namely $\tilde{x}(\lambda)$ and $\tilde{t}(\lambda)$, that are further assumed as solutions of equations (4) for some time interval $\lambda \in [0, \tilde{T}]$. For those solutions we can write $\tilde{x}(\lambda) = x(2t/\sqrt{a})$ as long as both sides of (4) are explicitly defined, that is, as long as the solutions for x and \tilde{x} differ only by an arbitrary constant. This constant, in essence, is just a rescaling of the time (Nair, 2012; Kosmas and Vlachos, 2016).

In exploring for appropriate expressions for $\tilde{x}(\lambda)$ and $\tilde{t}(\lambda)$, we consider the two Lagrangians

$$L_1 = \sqrt{x'^2 + f(x)t'^2}, \quad L_2 = \frac{1}{2}(x'^2 + f(x)t'^2) \quad (5)$$

The action corresponding to L_1 is invariant under arbitrary reparametrization of λ , whereas the L_2 action is only affine reparametrization invariant. This leads to Euler-Lagrange equations corresponding to L_2 that are affine time reparametrization invariants.

The Euler-Lagrange equations that come out of L_1 are

$$\frac{d}{d\lambda} \left(\frac{x'}{\sqrt{x'^2 + f(x)t'^2}} \right) = \frac{t'^2}{2\sqrt{x'^2 + f(x)t'^2}} \frac{\partial f}{\partial x} \quad (6a)$$

$$\frac{d}{d\lambda} \left(\frac{f(x)x'}{\sqrt{x'^2 + f(x)t'^2}} \right) = 0. \quad (6b)$$

The later equations are also reparametrization invariants with respect to λ , i.e. they are invariant under the replacements $\lambda = \lambda(\mu)$ and $d\lambda/d\mu \neq 0$, which means that, a solution of (6) defines a curve in the space (x, t) . Furthermore, this solution gives us information on which curve does it belong, but it does not show us the exact point at that curve. The curve in question acts as a geodesic information for the system of equations as well as for its solution. The later equations are then considered to be evolution equations, which provide us with, not only the shape of the curve, but also with its parametrization (Kosmas and Vlachos, 2016).

In order to understand more deeply the latter conclusions, we find it helpful for the reader to proceed with an example of a specific numerical scheme, which, as mentioned above, is chosen here to be the high order exponential variational integrators (Kosmas and Vlachos, 2010; Kosmas and Leyendecker, 2016; Kosmas and Leyendecker, 2019).

III. THE ADVANTAGES OF EXPONENTIAL VARIATIONAL INTEGRATORS

The derivation of high order variational integrators, applicable for physical systems where the Lagrangian is of separable form, come out of similar techniques to those employed in the theory of discrete variational calculus, see e.g. (Marsden and West, 2001). To that end, for a smooth and finite dimensional configuration manifold Q , one defines the discrete Lagrangian

$$L_d: Q \times Q \rightarrow \mathbb{R}. \quad (7)$$

This Lagrangian may be considered as an approximation of a continuous action obtained as

$$L_d(q_k, q_{k+1}, h_k) \simeq \int_{t_k}^{t_{k+1}} L(q, \dot{q}) dt. \quad (8)$$

Then the action sum $S_d: Q^{N+1} \rightarrow \mathbb{R}$, with $N \in \mathbb{N}$, that corresponds to the above Lagrangian is defined as

$$S_d(\gamma_d) = \sum_{k=0}^{N-1} h_k L_d(q_k, q_{k+1}, h_k), \quad (9)$$

where $\gamma_d = (q_0, \dots, q_N)$ denotes the discrete trajectory of the studied system (and h_k the k^{th} time step). Following the procedure of the continuous settings we can further compute the derivative of L_d as

$$dL_d(q_0, q_1) = D_1 L_d(q_0, q_1) + D_2 L_d(q_0, q_1), \quad (10)$$

interpreting $D_1 L_d$ for the derivative with respect to the i -argument of L_d . According to the discrete variational principle, the solutions of the discrete system are determined from L_d by extremizing the action sum keeping the endpoints q_0 and q_N fixed. Extremizing S_d over all the intermediate points of γ_d , the obtained system of difference equations is

$$h_{k-1} D_2 L_d(q_{k-1}, q_k, h_{k-1}) + h_k D_1 L_d(q_k, q_{k+1}, h_k) = 0. \quad (11)$$

This discrete version of the continuous Euler-Lagrange equations are known as discrete Euler-Lagrange equations (Marsden and West, 2001; Kosmas and Vlachos, 2010).

To derive high order methods addressed in this work, we approximate the action integral along the curve segment between q_k and q_{k+1} using a discrete Lagrangian that depends only on the end points, see Eq. (8). This way, we obtain expressions for the configurations q_k^j and velocities $\dot{q}_k^j, j = 0, \dots, S-1, S \in \mathbb{N}$, at time $t_k^j \in [t_k^j, t_{k+1}^j]$. Then, by expressing the t_k^j as $t_k^j = t_k + C_k^j h_k$ for $C_k^j \in [0, 1]$ such that $C_k^0 = 0, C_k^1 = 1$, we write (Kosmas and Vlachos, 2010)

$$\begin{aligned} q_k^j &= g_1(t_k^j) q_k + g_2(t_k^j) q_{k+1}, \\ \dot{q}_k^j &= \dot{g}_1(t_k^j) q_k + \dot{g}_2(t_k^j) q_{k+1}. \end{aligned} \quad (12)$$

We next choose the functions

$$\begin{aligned} g_1(t_k^j) &= \sin\left(u - \frac{t_k^j - t_k}{h_k} u\right) \sin^{-1}(u), \\ g_2(t_k^j) &= \sin\left(\frac{t_k^j - t_k}{h_k} u\right) \sin^{-1}(u), \end{aligned} \quad (13)$$

to represent the oscillatory behavior of the solution. For the sake of continuity, the conditions

$$g_1(t_{k+1}) = g_2(t_k) = 0 \quad \text{and} \quad g_1(t_k) = g_2(t_{k+1}) = 1 \quad (14)$$

are required to be fulfilled (Kosmas and Leyendecker, 2012; Kosmas and Vlachos, 2012; Kosmas and Leyendecker, 2015).

It should be mentioned that for any different choice of interpolation, we define the discrete Lagrangian by a weighted sum of the form (Kosmas and Vlachos, 2010)

$$L_d(q_k, q_{k+1}, h_k) = \sum_{j=0}^{S-1} h_k w^j L(q(t_k^j), \dot{q}(t_k^j)), \quad (15)$$

where, as can be readily proved, it holds

$$\sum_{j=0}^{S-1} w^j (C_k^j)^m = \frac{1}{m+1}, \quad (16)$$

with $m=0, 1, \dots, S-1$ and $m=0, 1, \dots, N-1$ (Kosmas and Vlachos, 2010; Kosmas and Leyendecker, 2012). By applying the above interpolation technique in combination with the expressions of (13) and following the analysis of (Kosmas and Vlachos, 2010; Kosmas and Leyendecker, 2012), the parameter u entering equations (13) must be chosen to be $u = \omega h$. For problems involving a definite frequency ω (such as the harmonic oscillator), the parameter u can be easily computed. However, for the solution of orbital problems of the general N -body problem, where no unique frequency of the motion can be in general determined, a new parameter u must be defined by estimating the frequency of the motion for any moving point mass (Kosmas and Leyendecker, 2016; Kosmas and Leyendecker, 2019).

IV. TIME ADAPTIVE EXPONENTIAL VARIATIONAL INTEGRATORS

In this section we apply the steps followed in Section 3, in the Lagrangians L_1 and L_2 of equations (5). Using (15), for the length action given by L_1 , the corresponding discrete Lagrangian reads

$$L_{1d}(q_k, q_{k+1}, h_k) = \sum_{j=0}^{S-1} h_k w^j \sqrt{(x_k^{\prime j})^2 + f(x_k^j)(t_k^j)^2}, \quad (17)$$

where the x_k^j are defined using (12) and $x_k^{\prime j}$, t_k^j using the expression

$$q_k^{\prime j} = \frac{\partial q_k^j}{\partial \lambda} = (\dot{g}_1(t_k^j)q_k + \dot{g}_2(t_k^j)q_{k+1}) \frac{\partial t}{\partial \lambda} = \dot{g}_1(t_k^j)q_k + \dot{g}_2(t_k^j)q_{k+1}. \quad (18)$$

For the Lagrangian (17), the discrete Euler-Lagrange equations (11) give the discrete analogues of (6a) as

$$\begin{aligned} & \sum_{j=0}^{S-1} w^j \frac{h_k}{2d_{k,k-1}} \left[2\dot{g}_2(t_k^j)(\dot{g}_1(t_k^j)x_{k-1} + \dot{g}_2(t_k^j)x_k) + \right. \\ & \left. \frac{\partial}{\partial x_k} f(g_1(t_k^j)x_{k-1} + g_2(t_k^j)x_k)(\dot{g}_1(t_k^j)t_{k-1} + \dot{g}_2(t_k^j)t_k)^2 \right] + \\ & \sum_{j=0}^{S-1} w^j \frac{h_{k+1}}{2d_{k+1,k}} \left[2\dot{g}_1(t_k^j)(\dot{g}_1(t_k^j)x_k + \dot{g}_2(t_k^j)x_{k+1}) + \right. \\ & \left. \frac{\partial}{\partial x_k} f(g_1(t_k^j)x_k + g_2(t_k^j)x_{k+1})(\dot{g}_1(t_k^j)t_k + \dot{g}_2(t_k^j)t_{k+1})^2 \right], \end{aligned} \quad (19)$$

and of (6b) as

$$\begin{aligned} & \sum_{j=0}^{S-1} w^j \frac{h_k \dot{g}_2(t_k^j)}{d_{k,k-1}} \left[f(g_1(t_k^j)x_{k-1} + g_2(t_k^j)x_k)(\dot{g}_1(t_k^j)t_{k-1} + \dot{g}_2(t_k^j)t_k)^2 \right] + \sum_{j=0}^{S-1} w^j \frac{h_{k+1} \dot{g}_1(t_k^j)}{d_{k+1,k}} \left[f(g_1(t_k^j)x_k + \right. \\ & \left. g_2(t_k^j)x_{k+1})(\dot{g}_1(t_k^j)t_k + \dot{g}_2(t_k^j)t_{k+1})^2 \right], \end{aligned} \quad (20)$$

In the latter equation $d_{k+1,k}$ is given by

$$d_{k+1,k} = \left\{ [\dot{g}_1(t_k^j)x_k + \dot{g}_2(t_k^j)x_{k+1}]^2 + f(g_1(t_k^j)x_k + g_2(t_k^j)x_{k+1})[\dot{g}_1(t_k^j)t_{k-1} + \dot{g}_2(t_k^j)t_k]^2 \right\}^{\frac{1}{2}}, \quad (21)$$

and $d_{k,k-1}$ by

$$d_{k,k-1} = \left\{ [\dot{g}_1(t_k^j)x_{k-1} + \dot{g}_2(t_k^j)x_k]^2 + f(g_1(t_{k-1}^j)x_{k-2} + g_2(t_{k-1}^j)x_{k-1})[\dot{g}_1(t_{k-1}^j)t_{k-2} + \dot{g}_2(t_{k-1}^j)t_{k-1}]^2 \right\}^{\frac{1}{2}}, \quad (22)$$

In accordance with the continuous case, equations (19) and (20) are not independent. To solve the system above, we can choose arbitrary step sizes in either t or x direction and solve these equations for the x or t , respectively.

Once the discrete Euler-Lagrange equations (19) and (20) are solved, we get a sequence of points $(x_0, t_0), \dots, (x_N, t_N)$, where t_0, \dots, t_N does not necessarily represent the physical time. Using this sequence of points, for the discrete Hamiltonian (Nair, 2012; Kosmas and Vlachos, 2016)

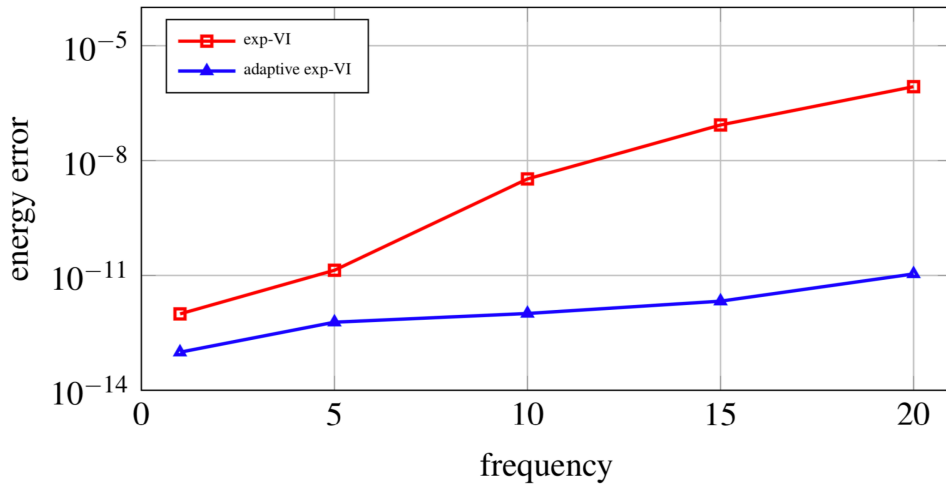
$$H_d(x_0, x_1, h_0) = -h_0 D_3 L_d(x_0, x_1, h_0) - L_d(q_0, q_1, h_0), \quad (23)$$

and recalling that the energy expressed by the Hamiltonian is conjugate variable of the physical time, i.e.

$$H_d(x_0, x_1, h_0) = H_d(x_2, x_2, h_1) \quad (24)$$

we can restore the physical time.

Figure1. Energy error for the harmonic oscillator using trigonometric interpolation (Section 3) versus the time adaptive one (Section 4) for the frequencies $\omega = 1, 5, 10, 20$.



V. NUMERICAL RESULTS

5.1 Harmonic oscillator

We will first test the proposed numerical scheme in the case of the simple pendulum described through the Lagrangian

$$L(q, \dot{q}) = \frac{1}{2} \dot{q}^2 - \frac{1}{2} \omega^2 q^2, \quad (25)$$

which leads to the equation of motion

$$\ddot{q} = -\omega^2 q. \quad (26)$$

Using the interpolation of (12), the discrete Lagrangian governing its motion takes the form

$$L_d(q_k, q_{k+1}) = \frac{h}{2} \left[\sum_{j=0}^{S-1} w^j (\dot{g}_1(t_k^j) q_k + \dot{g}_2(t_k^j) q_{k+1})^2 - \omega^2 \sum_{j=0}^{S-1} w^j (g_1(t_k^j) q_k + g_2(t_k^j) q_{k+1})^2 \right], \quad (27)$$

For this discrete Lagrangian, following Section 4, the discrete Euler-Lagrange equations provide the two-step variational integrator (Kosmas and Vlachos, 2012; Kosmas and Leyendecker, 2019)

$$q_{k+1} + \frac{\sum_{j=0}^{S-1} w^j [\dot{g}_1(t_k^j)^2 + \dot{g}_2(t_k^j)^2 - \omega^2 (g_1(t_k^j)^2 + g_2(t_k^j)^2)]}{\sum_{j=0}^{S-1} w^j [\dot{g}_1(t_k^j) \dot{g}_2(t_k^j) - \omega^2 g_1(t_k^j) g_2(t_k^j)]} q_k + q_{k+1} = 0, \quad (28)$$

In order to demonstrate the benefits of the proposed technique on the numerical accuracy of the obtained methods, we test the performance by comparing the methods of Section 3 with the ones proposed in Section 4. Towards this purpose, we check the energy error at a specific integration time $t = 3$ (arbitrary taken) for five different frequencies $\omega \in \{1, 5, 10, 15, 20\}$ and initial conditions $(q_0, p_0) = (2, 1)$, see Figure 1. As can be seen both methods increase the energy error as the frequency of the problem increases. Secondly, although for relatively small choices of $\omega < 5$ both methods lead to energy error smaller than about 10^{-11} , for high frequency values, constant time step schemes lead to clearly larger energy error.

In computing the above results, both methods were considered to be third order methods, i.e. $S = 4$, while similar results have been obtained for other choices of S . We should also note that, we have chosen the same initial time step $h = 0.05$ for all results of Figure 1.

In order to illustrate how the time step change effectively the computational cost, which was one of the main purposes of our present work, we consider below a more complicated example.

5.2 The two-body problem

In the known Kepler's problem (also called the two-body problem), two objects are interacting through a central force field. By choosing one of the bodies as the centre of the coordinate system, the resulting motion is a planar one. Assuming (whithout loss of generality) that masses and gravitational constant are equal to 1, we denote the position of the moving body by $q = (q_1, q_2)^T$. Then the Lagrangian of the system takes the form

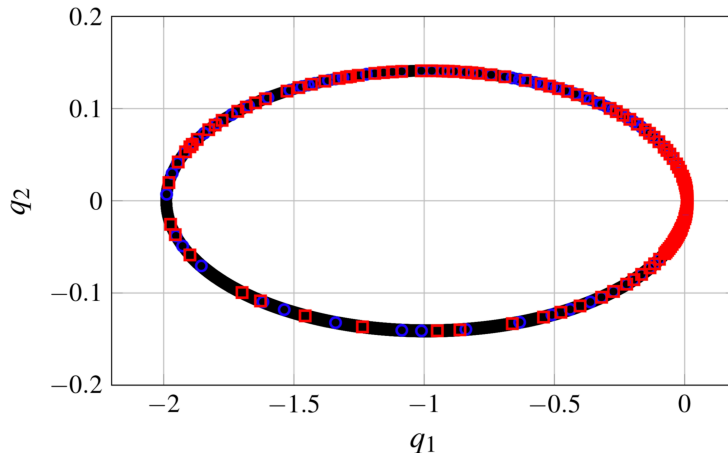
$$L(q, \dot{q}) = \frac{1}{2} \dot{q}^T \dot{q} + \frac{1}{|q|}, \quad (29)$$

The initial conditions are taken appropriately as in (Hairer, 1997)

$$q = (1 - \varepsilon, 0)^T, \quad \dot{q} = \left(0, \sqrt{\frac{1+\varepsilon}{1-\varepsilon}} \right)^T, \quad (30)$$

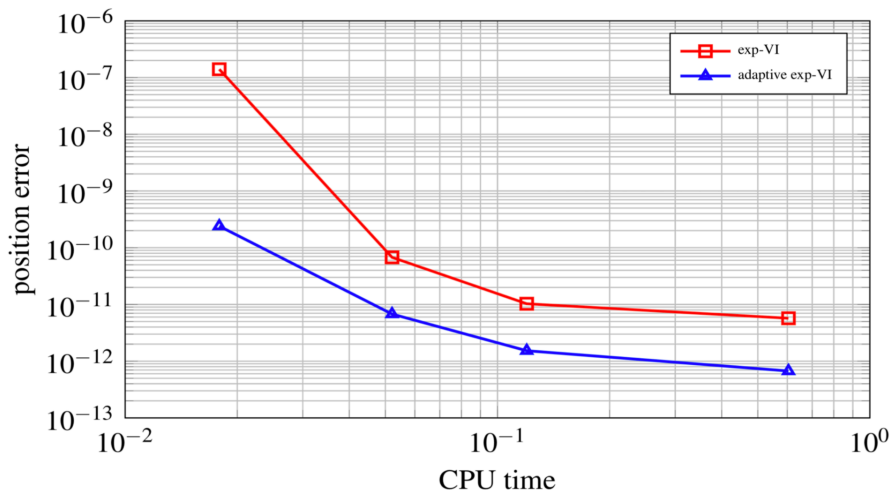
where ε is the eccentricity of the elliptical trajectory of the orbiting object. To check the efficiency of the proposed technique, we consider here only orbits with remarkably high eccentricities ($\varepsilon = 0.99$) and test the performance by comparing the methods of Section 3 with the ones proposed in Section 4 for long term integrations, i.e. for 10^6 periods. Figure 2 shows the exact orbit obtained with the method of Section 3 (solid line), the calculated points for the first period (points labeled with \circ) and the calculated points for the last period (points labeled with \square). While most of the standard symplectic schemes fail to track the orbit for such a high eccentricity (among them the one discussed in Section 3, see (Hairer, 1997), when adaptive time step is considered, the resulting integrator is remarkably stable keeping the orbit close to the exact one. For this numerical experiment the observed energy error is oscillating around much smaller values, i.e. around 10^{-7} .

Figure2. Exact solution of the 2-body problem for 10^6 periods and for eccentricity 0.99 (solid line). Calculated points for the first (\circ) and last period (\square) using adaptive exponential variational integrators of Section 4.



Finally, in order to explore the numerical convergence of the proposed method, we choose as initial conditions $(q_0, p_0) = (2, 2)$ and the time interval $[0, 3]$ (Kosmas and Leyendecker, 2019). We first calculate the global errors for the position at $t = 3$ (arbitrary taken, but following Stern, 2009; Kosmas and Leyendecker, 2019) whereas using constant time steps $h \in \{0.01, 0.05, 0.1, 0.5, 1\}$. Figure 3 shows the above errors versus the computational time needed to obtain them (red line). It is obvious that smaller position errors are obtained for short time steps, which leads to bigger computational time. When the adaptive time step method of Section 4 was applied (blue line), the position error obtained was remarkably smaller. It should be mentioned that, in obtaining these results, we forced the proposed schemes to take the same computational time with the ones taken for constant time step.

Figure3. Position error for the 2-body problem for eccentricity 0.99 at an arbitrary taken time $t = 3$ for the exponential integrators with constant time step (red line) versus the one that uses adaptive time step (blue line).



VI. CONCLUSIONS

In the present paper, an approach for deriving high order exponential variational integrators with adaptive time step has been developed. Focusing on systems of which the Lagrangian is of separable form, the proposed technique unfolds the standard Euler-Lagrange character to its space-time manifold and translates it through the geodesic (shortest route) connecting two points. From the adaptive time step methods addressed here, rather than optimizing the choice of step sizing, we introduce an artificial time step parameter, and use the energy behaviour in order to calculate the actual one.

Simulation tests showed that, this technique integrates efficiently stiff systems (like the two body problem with very high eccentricity up to 0.99) while conserving at the same time all the benefits of the classical variational integrators.

Conflict of interest

There is no conflict to disclose.

REFERENCES

- [1]. Marsden, J.E., Patrick, G., Shkoller, S., 1998. Multisymplectic geometry, variational integrators, and nonlinear pdes, *Comm. Math. Phys.* 199, 351.
- [2]. Hairer, E., 1997. Variable time step integration with symplectic methods, *Applied Numerical Mathematics* 25, 219.
- [3]. Kane, C., Marsden, J.E., Ortiz, M., (1999). Symplectic energy-momentum preserving variational integrators, *J. Math. Phys.* 40, 3353.
- [4]. Leok, M., Zhang, J., 2011. Discrete Hamiltonian variational integrators. *IMA J. Numer. Anal.* 31, 1497.
- [5]. Ober-Bloebaum, S., Saake, N., 2015. Construction and analysis of higher order Galerkin variational integrators. *Advances in Computational Mathematics* 41, 955.
- [6]. Skeel, R.D., 1993. Variable step size destabilizes the Störmer/leapfrog/Verlet method, *BIT Numerical Mathematics* 33, 172.
- [7]. Calvo, M.P., Sanz-Serna, J.M., 1993. The development of variable-step symplectic integrators, with application to the two-body problem, *SIAM J. Sci. Comput.* 14, 936.
- [8]. Wright, J.P., 1998. Numerical instability due to varying time steps in explicit wave propagation and mechanics calculations, *Journal of Computational Physics* 140, 421.
- [9]. Reich, S., 1999. Backward error analysis for numerical integrators, *SIAM Journal on Numerical Analysis* 36, 1549.
- [10]. Marsden, J.E., West, M., 2001. Discrete mechanics and variational integrators, *Acta Numerica* 10, 357.
- [11]. Stern, A., Grinspun, E., 2009. Implicit-explicit integration of highly oscillatory problems. *SIAM Multiscale Model. Simul.* 7, 1779.
- [12]. Kosmas, O.T., Vlachos, D.S., 2010. Phase-fitted discrete Lagrangian integrators, *Computer Physics Comm.* 181, 562.
- [13]. Kosmas, O.T., Leyendecker, S., 2016. Analysis of higher order phase fitted variational integrators, *Advances in Computational Mathematics* 42, 605.
- [14]. Kosmas, O.T., Leyendecker, S., 2019. Variational integrators for orbital problems using frequency estimation, *Advances in Computational Mathematics* 45, 1-21.
- [15]. Nair, S., 2012. Time adaptive variational integrators: A space-time geodesic approach, *Physica D: Nonlinear Phenomena* 241, 315.
- [16]. Kosmas, O.T., Vlachos, D.S., 2016. A space-time geodesic approach for phase fitted variational integrators, *Journal of Physics: Conference Series* 738.
- [17]. Kosmas, O.T., Leyendecker, S., 2012. Phase lag analysis of variational integrators using interpolation techniques, *PAMM Proc. Appl. Math. Mech.* 12, 677.
- [18]. Kosmas, O.T., 2011. Charged particle in an electromagnetic field using variational integrators, *ICNAAM Numerical Analysis and Applied Mathematics* 1389, 1927.
- [19]. Kosmas, O.T., 2019. Exponential variational integrators for the dynamics of multibody systems with holonomic constraints, *Journal of Physics: Conference Series* 1391.
- [20]. Kosmas, O.T., Leyendecker, S., 2015. Family of higher order exponential variational integrators for split potential systems, *Journal of Physics: Conference Series* 574.
- [21]. Kosmas, O.T., Papadopoulos, D., 2014. Multisymplectic structure of numerical methods derived using nonstandard finite difference schemes, *Journal of Physics: Conference Series* 490.

Odysseas Kosmas. " Analysis of adaptive higher order exponential variational integrators." *International Journal of Engineering and Science*, vol. 10, no. 10, 2020, pp. 57-63.